HAIT Journal of Science and Engineering A, Volume 5, Issues 1-2, pp. 52-70

Disorder effects in dilute magnetic semiconductors

Boris A. Aronzon

Russian Research Center "Kurchatov Institute",
Kurchatov sq. 1, Moscow 123182, Russia
and
P.N. Lebedev Research Center in Physics,
Leninskii Ave. 53, Moscow 119991, Russia
e-mail: aronzon@mail.ru

Received 22 August 2007

Abstract

The paper summarizes the results of our studies of disorder effects in dilute magnetic semiconductors. The structural, magnetic and Coulomb disorder are discussed both in bulk and 2D systems. The magnetic and transport properties of structures with MnSb ferromagnetic nanograins embedded into GaMnSb matrix, InGaAs quantum wells doped with Mn delta-layer separated from the quantum well by the 3 nm thick spacer and $CdGaAs_2$ bulk single crystal with 6 at% Mn are discussed.

PACS: 75.50.Pp, 71.55.Eq, 72.20.My, 72.25.Dc

1 Introduction

First time I. Vagner helped me in my investigations when I yet was not acquainted with him. I was invited in the Laboratoire National des Champs Magnétiques Pulsés (Toulouse) as a visiting researcher. The desk they provided useful for my studies. Then I recognized that before me this desk was used by I. Vagner, who stayed for some time in Toulouse and returned back

to Grenoble. We discussed some scientific problems by phone and eventually he invited me to visit him in the Laboratory of High Magnetic Fields in Grenoble. We agreed to meet in the restaurant nearby the Grenoble railway station. I asked him, "How I can recognize you?" And he answered "Do not worry, you will do". I was slightly surprised and disappointed, but when he entered the hall I really did. After that we discussed various topics and he explained his ideas how one could build a qubit using electron spins. That was the starting point of my studies of dilute magnetic semiconductors (DMS). This paper summarizes some of results of these investigations.

Creation of materials which demonstrate both ferromagnetic and semiconductor properties stimulated the new tendency in spintronics and as a result studies of diluted magnetic semiconductors (DMS) started to be a hot topic in modern condensed matter physics [1, 2]. The most popular materials are DMS based on III-V semiconductors doped with Mn. The discovery of ferromagnetism (FM) in (In,Mn)As with Curie temperature $T_C = 35$K and then in (Ga,Mn)As with $T_C = 60$K [3] stimulated a systematic study of DMS with non-cryogenic Curie temperatures. DMS are semiconductors, which contain up to 10% of magnetic impurities. It was shown [4] that in the case of $Ga_{1-x}Mn_xAs$ layers the optimal Mn concentration is of $x \approx 0.05 - 0.06$. Usually, single-phase single crystal films are formed with the help of the low-temperature molecular-beam epitaxy (LT-MBE) method. Curie temperature of about 110 K was achieved in these films with the hole concentration $p = 3.5 \cdot 10^{20}\text{cm}^{-3}$ [4]. Recently, the T_C value of around 160 K was achieved [5]; this value of T_C approaches a possible theoretical limit [6]. One of the main goals in DMS studies is to reach high T_C values, but Curie temperatures in (III,Mn)V DMS are limited by low solubility of Mn in III-V and by complexity of the LT-MBE technique.

There is a lot of unsolved problems related to DMS as new and perspective materials. One of these problems is the role of disorder in formation of DMS properties [7], and we address this problem in our paper. It is clear, that high concentration (several percent) of randomly distributed Mn causes a strong disorder in DMS materials. Usually Mn in III-V semiconductors acts not only as a magnetic impurity but also as an acceptor substituting for Ga ions. However, at high content Mn also enters interstitials, being a donor impurity in this position [2, 8]. Also at high content Mn forms grains consisting from Mn compound with V element, such as MnAs or MnSb, which are ferromagnetic metals. So there are at least three types of disorder which should be taken into account: structural (grains of a different phase), magnetic (non-uniform distribution of magnetic ions resulting in fluctuations of local magnetic moments) and electrical (non-uniform distribution

of charged impurities leading to fluctuation potential). We will discuss all three types of disorder in this paper.

Another unresolved problem is the mechanism of exchange in such materials. Although the microscopic mechanism of magnetic ordering in these materials is still under discussion, it is generally accepted that ferromagnetism is mediated by free and localized holes in the impurity band ("carrier-mediated ferromagnetism") [2]. This statement is proved by the observation of T_C dependence on charge carrier concentration at constant Mn content [9]. The magnetic disorder in DMS and in 2D structures based on such material could not be discussed without touching this problem, so we will do that as well.

2 Anomalous Hall effect in GaMnSb films and structural disorder

As it was mentioned above, compounds of Mn with V elements form at high values of Mn contents. These precipitates are present in DMS films as small metallic grains (mainly ferromagnetic). Such grains should be treated as one of the sources of disorder in DMS. This disorder and its influence on the DMS transport properties is discussed below on the basis of results obtained with GaSb:Mn films synthesized by laser plasma deposition (see also [10]). The films with the thickness $40-140$ nm were deposited on semi-insulating GaAs (100) substrates. The substrate temperature T_S was varied from 200^oC up to 440^oC resulting in the variation of the hole concentrations in the range of $p = 5 \cdot 10^{20}$ cm^{-3} - $3 \cdot 10^{19}$ cm^{-3}. We have found that the change of hole concentration more then by the order of magnitude keeps the value of a saturated magnetization roughly the same for all films in the range $M_S = 3.6 - 5.3$ mT. The high quality of the sample structure and the existence of the MnSb grains is easily seen from electron diffraction pattern presented at Fig. 1.

One of the most effective methods to study DMS structures and to detect the spin-polarized carriers is the anomalous Hall effect (AHE). It is known, that the Hall field E_H in magnetic materials consists of two components [11]

$$E_H = R_0 B j_x + R_a M j_x,$$

where B is magnetic induction, M is magnetization, j_x is current density, R_0 is coefficient of normal Hall effect caused by the Lorentz force, and R_a is coefficient of anomalous Hall effect.

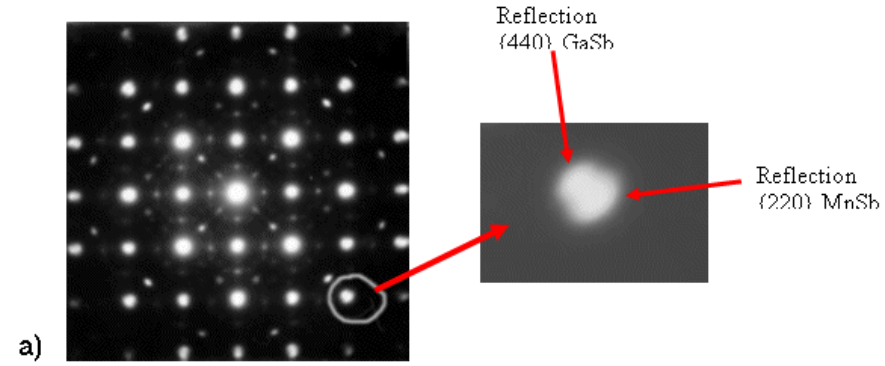

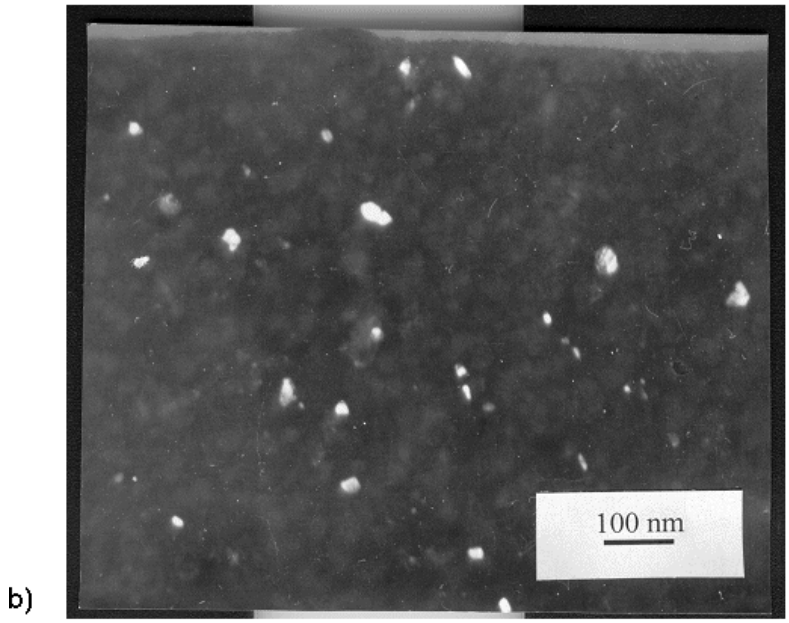

Figure 1: a) Electron diffraction pattern of (Ga,Mn)Sb sample and the zoom of its part showing the similiarity of the matrix reflexes {440} and MnSb reflexes {220}; b) Electron microscopic image of (Ga,Mn)Sb sample demonstrating the existence of grains in the matrix.

Contrary to the magnetization, characteristics of Hall effect depend crucially on the concentration of holes (on deposition temperature T_S). Fig. 2 depicts magnetic field dependences of the Hall resistance $R_{xy}(B)$, obtained

at $T = 77$ K (Fig. 2a) and $T = 293$ K (Fig. 2b) for GaSb:Mn samples with the hole concentrations $p = 5 \cdot 10^{20}$ cm^{-3} (curve 1), $p = 1.5 \cdot 10^{20}$ cm^{-3} (curve 2) and $p = 3{\cdot}10^{19}$ cm^{-3} (curve 3), respectively. The carrier concentration was evaluated from the slope of the curve $R_{xy}(B)$ at magnetic fields $B > 0.4 - 0.5$ T. Linear character of this dependence at high magnetic field is demonstrated by the insert in Fig. 2b for the sample 1. From Fig. 2, it is seen that the Hall effect in samples 1 and 2 is anomalous in the range of T=77-300 K, while in the sample 3 with the smallest hole concentration the Hall effect is ordinary. A comparison between data for samples 1 and 2, presented in Fig. 2, demonstrates that a decrease of the hole concentration suppresses the hysteretic behavior of AHE. Specifically, the coercitive force for the sample 1 ($p = 5 \cdot 10^{20}$ cm^{-3}) $B_C = 0.29$ T at $T = 77$ K and the hysteresis in AHE exists up to room temperature ($B_C = 6.5$ mT, see lower insert in Fig. 2b). At the same time, for the sample 2 ($p = 1.5 \cdot 10^{20}$ cm^{-3}) the value of $B_C = 0.058$ T at $T = 77$ K, and the hysteresis in AHE was not detected at $T = 300$ K.

Under the predominance of the AHE, the Hall resistance R_{xy}^S is proportional to spontaneous magnetization M_S. In this case a procedure, developed by A. Arrott [12], was proposed in [4, 13] for the determination of R_{xy}^S. This method for determination of R_{xy}^S value is a tool to minimize the effects of magnetic domain formation and magnetic anisotropy. To realize it, one has to plot the R_{xy}^2 dependence versus B/R_{xy} and extrapolate its linear part to intersection with ordinate axis for evaluation of R_{xy}^S.

Examples of R_{xy}^2 dependencies on B/R_{xy} at several measurement temperatures are shown in Fig. 3 for the sample 1. The linear extrapolation of the R_{xy}^2 values to $B = 0$ gives $(R_{xy}^S)^2 > 0$ for temperatures of 267 and 293 K, while at 335 K the linear extrapolation results in negative value of $(R_{xy}^S)^2$, suggesting that ferromagnetic ordering is absent at this temperature. The temperature dependences of coercitive field B_c and spontaneous Hall resistance R_{xy}^S, obtained by this method [12, 13], are shown in Fig. 4 for the sample 1. The presented data indicate that hysteresis loss temperature reaches $T_C \approx 330$ K in this sample. Similar procedure gives $T_C \approx 180$ K for the sample 2.

We are inclined to connect the observed results with the presence of ferromagnetic clusters. It was found [14] that, if the films are grown by high temperature MBE technique ($T_S = 560^o$C), the MnSb phase is dominant and all manganese atoms are situated in ferromagnetic MnSb clusters. Under these conditions, the normal Hall effect was predominant down to $T \approx 10$ K for GaSb:Mn sample with total Mn content of $x = 0.013$ and the hole

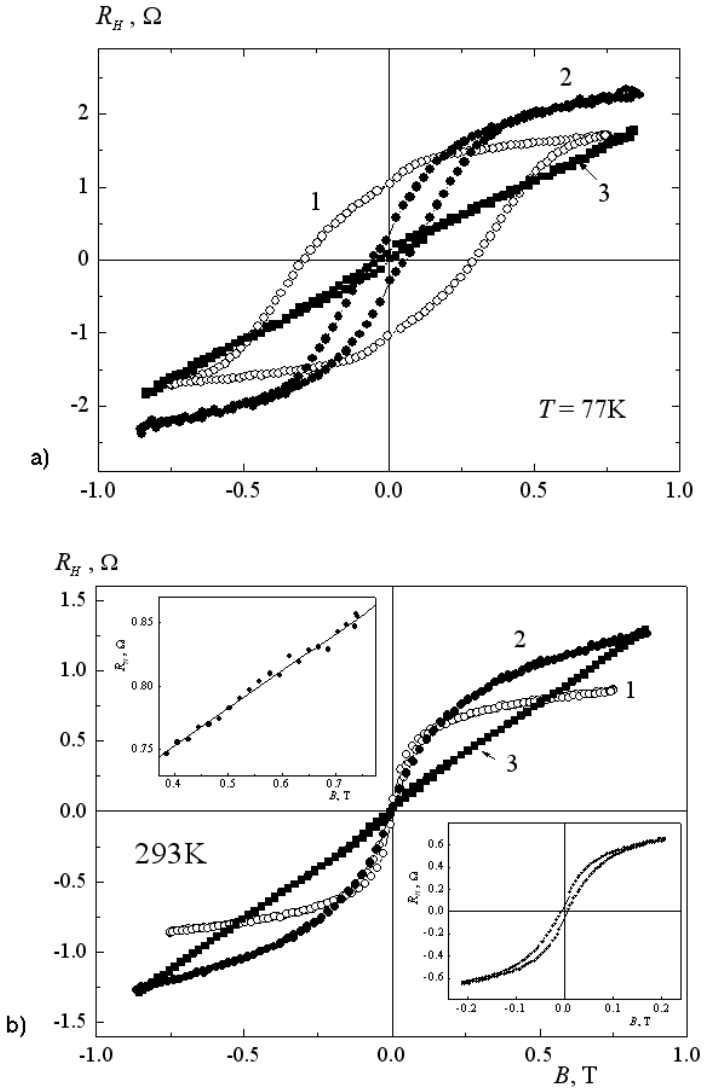

Figure 2: Hall resistance versus magnetic field for GaMnSb/GaAs structures: 1 - $p = 5 \cdot 10^{20}$ cm^{-3}, $T_S = 200^o$C; 2 - $p = 1.5 \cdot 10^{20}$ cm^{-3}, $T_S = 200^o$C; 3 - $p = 3 \cdot 10^{19}$ cm^{-3}, $T_S = 440^o$C. Measurement have been performed at temperatures: (a) 77 K; (b) 293 K. For (b) the upper inset is $R_H(B)$ dependence for the sample 1 at $B > 0.4$ T; the bottom inset is $R_{xy}(B)$ for the same sample 1 at $-0.2 < B < 0.2$ T.

concentration equal to $2.4 \cdot 10^{19}$ cm^{-3} [14]. On the other hand, the samples obtained at low temperature $T_S = 250^o - 300^o$C with Mn atoms located in Ga sites and practically containing no MnSb clusters exhibit the pronounced AHE with negative sign, which is opposite to that of normal Hall effect [14]. We have investigated samples with hole concentration close to that used in [14]. In our sample 3 with small hole concentration ($p = 3 \cdot 10^{19}$ cm^{-3}) Hall effect is normal like in analogous sample studied in [14]. However, hole concentration in this sample is essentially smaller then that in samples 1 and 2 and the results obtained for these samples differ drastically from those obtained in [14]. Critical temperature estimated by means of Arrot's procedure was $T_C \approx 25$ K for the sample with Mn content $x = 0.016$ and with $p = 1.3 \cdot 10^{20}$cm^{-3}. In contrast, our sample 2 having nearly the same concentration ($p = 1.5 \cdot 10^{20}$ cm^{-3}) shows $T_C \approx 180^o$ and positive sign of the AHE.

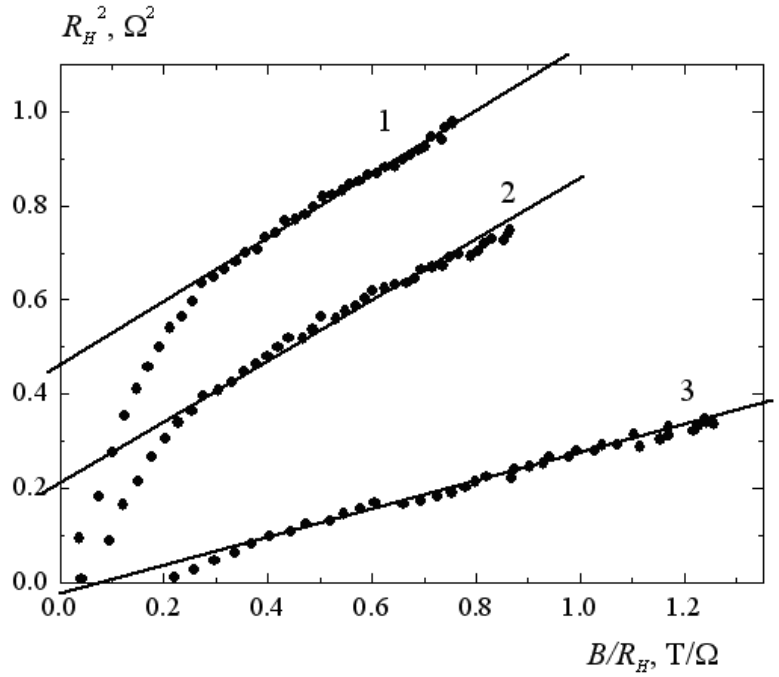

Figure 3: R_{xy}^2 values versus B/R_{xy} for the sample 1 ($p = 5 \cdot 10^{20}$ cm^{-3}). Measurements have been performed at temperatures: 1 - 267 K; 2 – 293 K; 3 – 335 K.

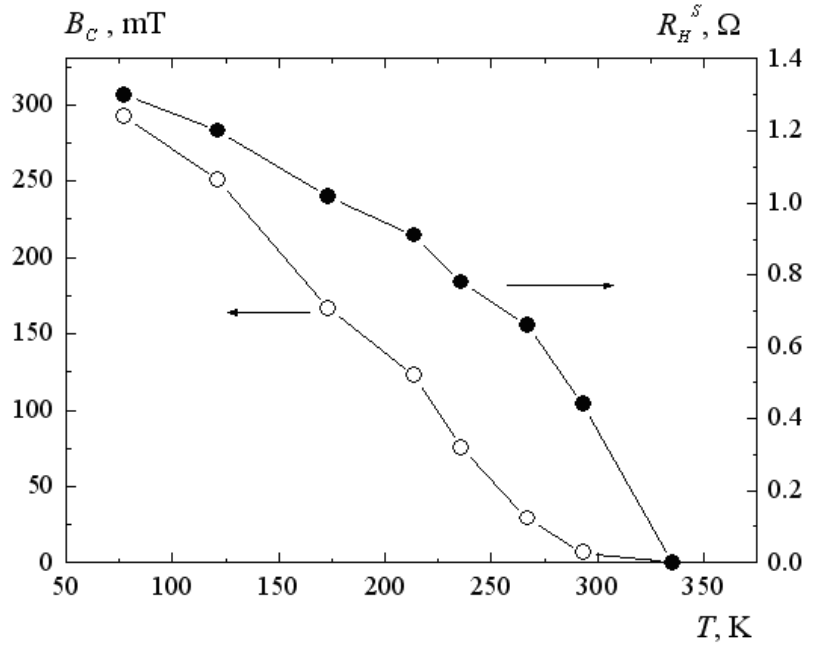

Figure 4: Temperature dependencies of coercive force B_C (left curve) and spontaneous Hall resistance component R_{xy}^S (right curve) for the sample 1.

Turning now to discussion of experimental data presented above, we note that the sign of AHE is positive in continuous MnSb films [15] like in our samples. It is reasonable to suggest that the AHE sign persists at transition from continuous film to discontinuous one. Such sign conservation we observed [16] for Fe nanoparticles in SiO_2 matrix at transition through percolation threshold to tunneling regime of conduction. It should be recognized, that our films, grown at temperatures of $T_S = 200 - 440^oC$ contain approximately identical concentrations of ferromagnetic phase as is seen from practical independence of magnetization data on T_S.

The above results suggest that the AHE revealed in investigated GaMnSb samples is related to presence of MnSb-type clusters. A fundamental difference between our samples and films with MnSb clusters studied in [14] is related to the hole concentration. In our case the hole concentration is essentially larger in GaSb matrix, than in MBE films [14]. This high concentration is associated with production of acceptor-like defects (most probably, antisites GaSb) during the film growth by the Laser Plasma Deposition

method. The strong dependence of the AHE on the carrier concentration at nearly constant contents of ferromagnetic phase (see Fig. 2) reinforces the suggestion that the above difference is due to carrier concentration. The interaction of free carriers with ferromagnetic inclusions in semiconductors is likely to be determined by presence of Schottky barriers on interfaces between clusters and matrix (in our case, on MnSb/GaSb interface). This interaction depends not only on the contents of ferromagnetic phase, but also on the hole concentration. Increase of carrier concentration value would cause the Schottky barrier width to decrease. Estimates indicate that the expected Schottky barrier width is equal to ≈ 2 nm at $p = 10^{20}$ cm^{-3}. On the other hand, the effective length l_ψ for decay of the heavy holes wave function of ($m_{hh} = 0.23m_0$) under barrier is evaluated to be about $1.3 - 2.5$ nm under these conditions, and it could be longer than the Schottky barrier width at $p = 10^{20}$ cm^{-3} and the height of the barrier $\varphi = (1/3) \cdot E_g$. These facts imply strong tunneling exchange between free carriers and ferromagnetic clusters. So the interaction is enhanced with the increase of carrier concentration and AHE appears or becomes more pronounced. The temperature, at which AHE hysteresis vanishes, often is interpreted as the blocking temperature [17], where the transition to superparamagnetic limit happens. Our estimates show that the blocking temperatures for MnSb clusters of size $a_C \approx 10$ nm is about 200 – 300 K in agreement with experimental data. On the other hand, it should be noted that interpretation of the AHE data in the context of isolated (non-interacting) MnSb clusters faces obvious problems. Indeed, the rise of deposition temperature T_S could lead to increase of the cluster sizes. High values of the coercitive force and sharp rise of magnetization curve in the range of hysteresis support the conclusion that clusters are of single domain structure. The latter means that coercitivity should increase with cluster sizes. Contrary to this, experimental data show the weakening of the AHE coercivity with rising T_S. Thus it is reasonable to conclude that the MnSb cluster size is less than 10 nm and they interaction is mediated by carriers in the GaSb:Mn matrix.

To conclude this chapter the following should be noted: the ferromagnetic properties of the overdoped material such as GaSb:Mn are determined to a large extent by formation of magnetic nanoclasters. Shottky barriers on their interfaces prevent the AHE in such material at not too high carrier concentration, whereas the AHE became more and more pronounced with increasing carrier concentration.

3 Disorder in 2D structures and Coulomb long-range fluctuation potential

Unlike bulk (III,Mn)V DMS, investigations of 2D DMS structures are still relatively rare [6, 18 - 21] because of difficulties with 2D layer magnetization measurements on a base of spurious contributions from a substrate. The majority of previous AHE studies in 2D DMS was performed with the Mn layer penetrated in the 2D conductivity channel [6, 18 - 20] resulting in low charge carrier mobility ($2 - 5$ cm^2/(V·s) [6]). Contrary to that, we present the results of studies of the 2D Quantum Well (QW) structures GaAs/δ<Mn>/GaAs/$In_xGa_{1-x}As$/GaAs with high enough carrier mobility (2000 cm^2/(V·s)). As is shown by X-ray measurements, the Mn δ-layer in our structures is well separated from the QW by the 3 nm spacer [22]. Nevertheless, the magnetic order arises, and it influences transport properties. Here we discuss how disorder affects such structure properties.

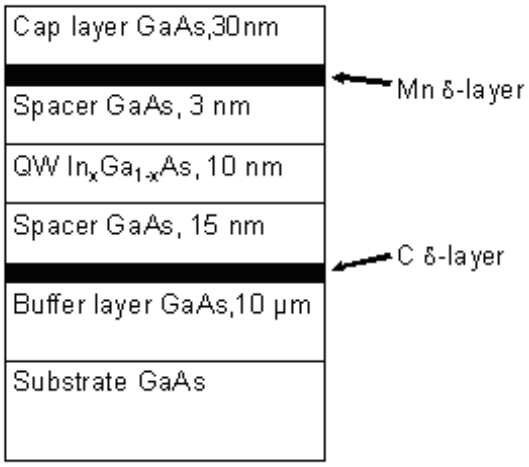

Figure 5: Schematic diagram of the structure.

The samples containing an $In_xGa_{1-x}As$ QW of width $d = 10$ nm inside a GaAs matrix were grown by MOS-hydride epitaxy. Magnetic properties of the samples are determined mainly by Mn δ-layer separated from the QW by a 3 nm thick spacer prepared by laser deposition. As is shown in our previous studies [21], the spacer thickness of 3 nm is the optimal one. That is because for thicker spacer the interaction between carriers inside QW and Mn δ-layer

is too weak, while for the thinner spacer Mn penetrates inside QW. Mn demonstrates mainly acceptor properties in GaAs, and our samples show the p-type conductivity. In addition to Mn δ-layer, the samples were doped with a C δ-layer from the buffer side. The scheme of our samples is shown in Fig. 5. The buffer layer and the spacers were grown at the temperature of 600^oC, while the deposition of Mn and cap layers was performed at 450 ^oC. Some technological and physical parameters of samples obtained by X-ray and transport measurements are presented in Table 1.

Table 1. Technological and physical parameters of the samples

Sample	x	d_{Mn}, ML	77 K		
			μ_{eff}, cm^2/(V·s)	$p_s \cdot 10^{-12}$, cm^{-2}	R_s, Ω/
A(M)	0.21	0.5	1860	2	1660
B(I)	0.16	1.8	1350	1.8	2540
C(I)	0.18	0	1598	0.5	7800

* (M stands for metallic and I for activation type of conductivity).

We have studied three different types of structures: (i) samples highly doped with Mn, (ii) samples with lower doping level, (iii) samples without Mn doping. The character of temperature dependence $R(T)$ of sample resistance is different for various samples at $T < 100$ K. As is seen from Fig. 6, the resistance of the sample with high Mn content (sample B, see Table 1) depends on temperature exponentially, apart from a kink around 30 K. On the other hand, the resistance of the sample with low Mn content (sample A) changes with the lowering temperature weakly (see Fig. 6). The metallic character of conductivity in this sample is proved by the detection of the very well pronounced Shubnikov-de Haas oscillations starting from 2 T. These oscillations will be discussed in another publication. So presented data look like the observation of the metal – insulator transition induced by the rise of Mn content. At first glance, it looks strange because Mn mainly acts as acceptor and carrier concentration should rise with increasing Mn content. However, as is seen from the Table 1 the hole concentration in samples A and B are nearly the same. The matter is that Mn ions at high concentration start to occupy interstitial sites acting as donors. It causes strong compensation which is typical for DMS [2]. For highly doped highly compensated semiconductors the metal – insulator transition due to strong long range fluctuation potential (FP) caused by compensation is well known and the relevant theory for 2D case was elaborated long ago [23]. Carriers are partly localized in wells of this potential thus forming metallic droplets

inside these wells. So in spite of high enough carrier mobility a disorder plays a very important role in our 2D DMS structures.

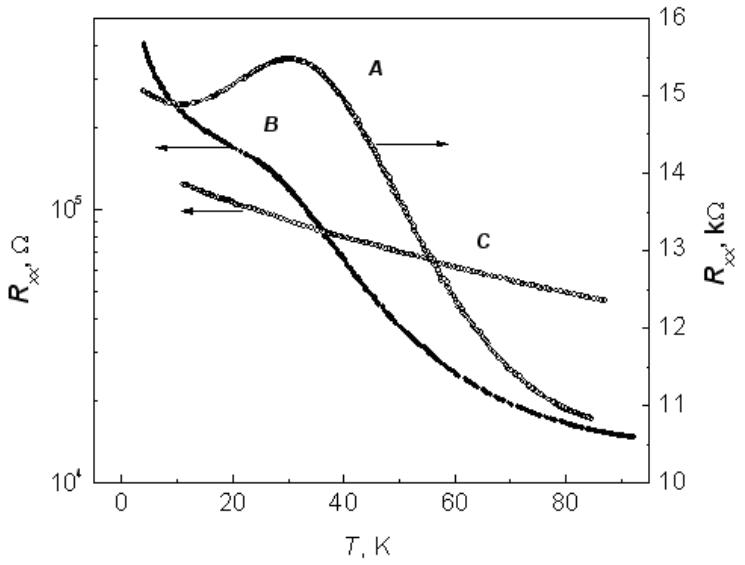

Figure 6: Temperature dependence of the sample resistance for the samples A, B and C.

Basing on the Gergel' – Suris theory [23] one could estimate the parameters of the fluctuation potential. The amplitude of the fluctuating potential γ is roughly equal to the energy gap between the percolation level and the Fermi level and therefore to the activation energy ε_a, $\gamma \approx \varepsilon_a = 10.5$ meV. The characteristic size of the potential well and thereby the size of metallic droplets is about the screening radius r_c [23]. To estimate r_c we compare the probability of hole activation on the percolation level, $w_a \sim \exp(-\gamma/kT)$, with the probability of tunneling between the hole droplets, $w_t \sim \exp(-2r_c/\lambda)$, where $\lambda = h/(2m^*\gamma)^{1/2}$ is the decay length of the wave function under the barrier of height defined by the energy difference between the percolation level and the Fermi level. Taking into account that the crossover from the activated conductivity of the carriers to tunneling between the FP wells takes place at $T_t = 24$ K one gets $r_c \approx 20$ nm, which is longer than the mean free path of the holes l_h. At $\mu \approx 10^3$ cm^2/V·s and $T \approx 30$ K we get $l_h \approx 6$ nm. Using the obtained value $r_c \approx 20$ nm and the holes concentration $p \sim 10^{12}$ cm^{-2} one can estimate $\gamma \sim 10 - 20$ meV, that is in agreement with $\varepsilon_a = 10.5$ meV.

So, 2D electrons dwell in a long range FP with high enough amplitude. This results in fragmentation of the 2d channel, which consists of lakes filled with holes (metallic droplets) and hills (insulating regions), which is usual for percolating systems.

The most impressive feature of the data presented in Fig. 6 is a kink on curves related to the Mn doped samples A,B, while in the resistance of the sample C without Mn this kink is absent. This behavior is natural for all magnetically ordered DMS and the temperature at which this kink is observed is widely considered as the Curie point T_C [1, 7]. There are several theories explaining the nature of this kink. According to the simplest of these theories, the scattering is spin-dependent, and the scattering rate is lower when all magnetic moments and spins of carriers are oriented in the same direction. At $T < T_C$ the scattering rate decreases, mobility increases that results in the rise of conductivity. This effect results in a kink for the experimental dependence of $R_{xx}(T)$ as we have observed.

To reinforce observed signs of magnetic ordering in the system we have performed AHE measurements. Up to now, AHE is the main tool for magnetization detecting in 2D DMS structures, because small values of their magnetic moments are difficult to extract from results of magnetometer measurements due to large diamagnetic contribution from the substrate [6, 20]. We determined R_0 in high magnetic fields taking into account that contrary to the AHE this component is not saturated in magnetic field. In our case, the normal component R_0 predominates, so special efforts were made to extract the AHE component. Finally we have succeeded to get for AHE conductivity $\sigma^a_{xy} \cong 0.07e^2/h$ for the sample A and $\sigma^a_{xy} \cong 0.17e^2/h$ for the sample B in agreement with recent theoretical calculation of AHE in 2D structures [24, 25], which gives $\sigma^a_{xy} \sim 0.1e^2/h$. The above mentioned calculations were performed taking into account the "intrinsic" mechanism model for the AHE origin [26]. According to the recent theoretical results, this is the main mechanism contributing to the AHE in DMS [26]. Theoretical results mentioned above [24, 25] were obtained assuming substantial spin polarization of the carriers. So we can conclude that very likely the carriers in our samples are spin polarized.

For insulating samples the above results are valid, of course, only at high enough temperatures, when the conductivity is determined by the carriers activated above the percolation level but not by the hopping mechanism. So the temperature dependence of the AHE in sample B is not monotonous, R^a_{xy} rises with the temperature lowering down to the temperature of crossover to the hopping conductivity $T_t = 24$ K, then R^a_{xy} drops down.

Next we turn to the results of magnetization measurements. These mea-

surements were performed with the help of SQUID magnetometer and with magnetic field aligned in the heterostructure plane. To extract contributions of the substrate and the sample holder we have measured magnetization of the sample holder without sample, then the sample under investigation (QW structure with Mn $\delta-$layer) was measured and after that measurements of QW structure without Mn $\delta-$layer were performed. Also the special procedure of the sample preparation for measurements was taken to avoid precipitation of microparticles on the sample surface. Subtracting contributions of the sample holder and of the sample substrate we have get the temperature and magnetic field dependencies of magnetic moment of the structure.

The magnetic field dependence of magnetic moment in the structure B (insulating one) is presented in Fig. 7. It should be noted that the data presented are the result of subtraction of parasitic signals. This is the reason for the small difference between the left and right parts of the curves.

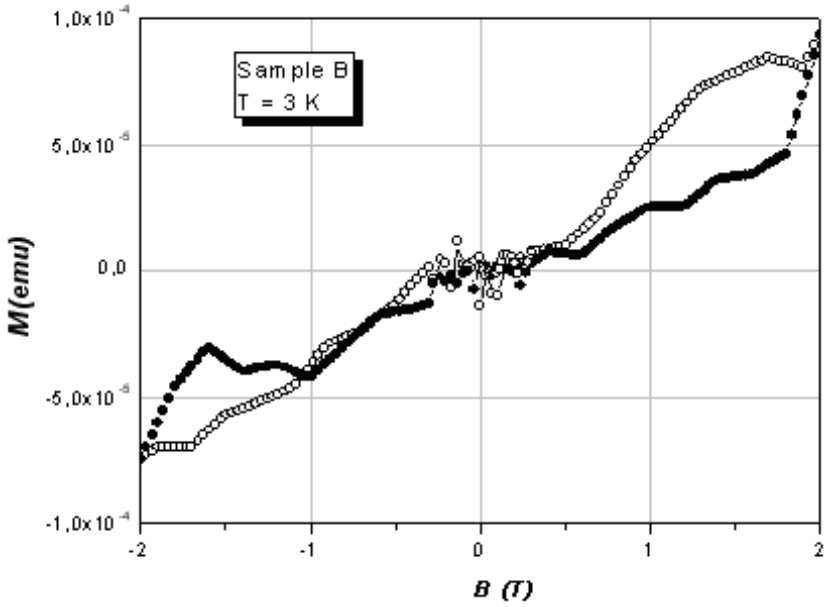

Figure 7: Magnetic field dependence of magnetic moment in the sample B.

The curve shown in Fig. 7 is quite unusual. The weak field dependence is related to that known for paramagnetic materials. On the other hand, at high fields the magnetic hysteresis is observed being the sign of ferromagnetic ordering. It should be noted that the hysteresis loop is shifted from

zero to higher values of magnetic field. For example, in the sample B the hysteresis loop is actually seen at $B > B_h \approx 1$ T. Such behavior is in agreement with the temperature dependence of magnetization. Really for sample B ZFC (Zero Field Cooled) and FC (Field cooled) curves coincide at fields above $B_h \approx 1$ T as it should be in the ferromagnetic state. On the other hand, above mentioned peculiarities are absent in the sample A with lower Mn concentration and the temperature dependence of the magnetization for this sample also correspond to spin-glass behavior at $T \leq 20$ K. This result does not contradict to the data obtained for sample B. The difference is due to the fact that the Mn content in the sample B is higher resulting in higher value of B_h, while the measurements were performed at the same field in both samples. Apparently, the field at which measurements were performed was not enough to induce ferromagnetic ordering in sample A. Such unusual magnetic properties and, in particular, the shifted hystersis loop were observed in systems containing both ferro- and antiferromagnetic regions (see [27, 28] for such results in DMS and imanganites, respectively). To interpret the obtained results one should assume the coexistence of ferro- and antiferromagnetic regions within the sample. The strong interaction between ferro- and antiferromagnetic regions keeps the orientation of the magnetic moment of the ferromagnetic region up to some field B_t at which the interaction of magnetic moments with an external field overcomes the interaction between grains, or exceeds the temperature of measurements, or at last the antiferromagnetic – ferromagnetic transition occurs at this field inside the antiferromagnetic islands. In case of weak interaction between ferromagnetic regions the random distribution of orientation of their magnetic moments should result in a superparamagnetic behavior under action of an external magnetic field. Thus, if the sample contains randomly distributed ferro- and antiferromagnetic grains interacting with each other, one should observe paramagnetic behavior at fields below B_t. At higher fields the ferromagnetic behavior changes for the paramagnetic one. As far as we know, the presented data are the first observation of exchange biased hysteresis loop in 2D structures.

4 ESR measurements and exchange mechanism

In the previous section we discussed the properties of 2D DMS structure related to exchange interaction involving carriers and magnetic ions separated from each other by 3nm spacer. This interaction arises in spite of the fact that the magnetism in DMS is known to be “carrier mediated” [2]. Up

to this moment we did not discuss the mechanism of the possible exchange, and we turn to this problem now. There is a lot of publications discussing the nature of the exchange mechanism in DMS [2]. However the final consensus is still not achieved. The suggested models could be divided in three different main assumptions: RKKY mechanism and its modifications [29], Zener mechanism and its modifications [29] and models taking into account electron transitions (possibly virtual) to extended or excited states [6]. The latter model could be responsible for the carrier mediated magnetism in case when carriers are spatially separated from magnetic ions. We call it "kinematic exchange" following [6]. To verify its importance, we present below results of the ferromagnetic exchange observation in the absence free carriers (to rule out RKKY exchange). We also show that this exchange is due to Mn in acceptor state (which have extended or excited states) but not to the neutral Mn states (to exclude conventional Zener mechanism). For this sake we have studied $CdGeAs_2$ doped with Mn. Mn can substitute both Cd, thus forming neutral states (since Cd is isovalent to Mn), and Ge forming Mn^{2+} + 2p acceptor states. Only one of these positions apparently possesses acceptor properties, which makes manganese a self-contained impurity for theformation of a ferromagnetic state in accordance with recent theoretical predictions [6].

III-V and II-IV-V_2 semiconductors are closely related structurally and are also isovalent: the valence per atom for valence of the II-IV complexes is equal to that of the III atoms. Mn doped single crystals of $CdGeAs_2$ have been synthesized by a chemical technology. In single-crystal with manganese concentration 6 mole % the study of thermopower and careful Hall measurements have revealed p-type carriers with density 6.5x10^{15} cm^{-3} at room temperature (RT). High mobility of p-holes with μ = 270 cm^2/V-s at the maximum at 175K (μ = 160 cm^2/Vs at RT) and activation energy E_a = 175 meV have been detected. So RKKY mechanism is not actual for such structures.

Magnetic properties of the crystal were studied by ESR and magnetization measurements and described in details in [30]. It was concluded from the data on the temperature dependence of the linewidth and reciprocal magnetic susceptibility χ (per Mn ion) that solely Mn atoms which substitute Ge and act as acceptor impurities are responsible for ferromagnetic exchange, while other ones do not contribute to the magnetic properties.

These data support the possibility for ferromagnetism governed by the recently proposed mechanism of exchange, called the kinematic exchange, [6]. According to this theory, an indirect exchange between Mn^{2+} + $2p$ complexes occurs via empty states near the top of the valence band due to

virtual excitation of electrons to excited extended electron states. So, only Mn ions "dressed" by holes could contribute to exchange while the neutral Mn atoms remain passive. This result is in the strong agreement with our experimental picture.

At low temperatures the sample demonstrates linear temperature dependence of χ^{-1} with Neel temperature about -6 K, while at temperatures higher 250 K χ^{-1} follows the Curie-Weiss law with the Curie temperature $T_C = 225$ K as it should be for ferromagnetic exchange [30]. One of the possible explanations is related to magnetic disorder due to non-uniform distribution of Mn atoms. In the regions rich with Mn the ferromagnetic exchange gives the main contribution down to the local Curie temperature. At lower temperatures each of these regions acts as small magnetic droplets. These superparamagnetic particles interact antiferromagnetically with each other, so that the observed behavior gets its natural explanation [30].

To conclude this part of the paper we should note that the obtained experimental results could be explained in the frame of the kinematic model of the exchange interaction and that the disorder plays a significant role in the manifestation of magnetic properties of DMS.

5 Conclusion

As a conclusion for the whole paper I would like to express my deep gratitude to Israel Vagner.

References

[1] Byounghak Lee, T. Jungwirth, and A.H. MacDonald, Semicond. Sci. Technol. **17**, 393 (2002); F. Matsukura, D. Chiba, Y. Ohno, T. Dietl, and H. Ohno, Physica E **16**, 104 (2003); I. Žutič, O. Fabian, S. Das Sarma, Rev. Mod. Phys. **76**, 323 (2004).

[2] T. Jungwirth, J. Sinova, J. Mašek *et al.*, Rev. Mod. Phys. **78**, 809 (2006).

[3] H. Ohno, H. Munekata, T. Penney, S. von Molnar, and L.L. Chang, Phys. Rev. Lett. **68**, 2664 (1992); H. Munekata, A. Zaslavsky, P. Fumagalli, R.J. Gambino, Appl. Phys. Lett. **63**, 2929 (1993); H. Ohno, A. Shen, F. Matsukura, A. Oiwa, A. Endo, S. Katsumoto, and Y. Iye, Appl. Phys. Lett. **69**, 363 (1996).

[4] F. Matsukura, H. Ohno, A. Shen, Y. Sugawara, Phys. Rev. B **57**, 2037 (1998).

[5] D. Chiba, K. Takamura, F. Matsukura, and H.Ohno, Appl. Phys. Lett. **82**, 3020 (2003); K.W. Edmonds, P. Boguslawski, K.Y. Wang, R.P. Campion, N.R.S. Farley, B.L. Gallagher, C.T. Foxon, M. Sawicki, T. Dietl, M.B. Nardelli, and J. Bernholc, Phys. Rev. Lett. **92**, 037201 (2004).

[6] P.M. Krstajič, F.M. Peeters, V.A. Ivanov, V. Fleurov, and K. Kikoin, Europhys. Lett. **61**, 235 (2003); Phys. Rev. B **70**, 195215 (2004).

[7] C. Timm, J. Phys.: Condens. Matter **15**, R1865 (2003).

[8] E. Abe, F. Matsukura, H. Yasuda, Y. Ohno, and H. Ohno, Physica E **7**, 981 (2000).

[9] A.M. Nazmul, S. Sugahara, and M. Tanaka, Phys. Rev. B **67**, 241308R (2003); A.M. Nazmul, T. Amemiya, Y. Shuto *et al.*, Phys. Rev. Lett. **95**, 017201 (2005).

[10] V.V. Rylkov, B.A. Aronzon, Yu.A. Danilov, Yu.N. Drozdov, V.P. Lesnikov, K.I. Maslakov, and V.V. Podolskii, JETP **100**, 742 (2005).

[11] See e.g. *The Hall Effect and Its Applications*, Eds: C.L. Chien and C.R. Westgate (Plenum, N.Y., 1980).

[12] A. Arrott, Phys. Rev. **108**, 1394 (1957).

[13] F. Matsukura, D. Chiba, T. Omiya *et al.*, Physica E **12**, 351 (2002).

[14] E. Abe, F. Matsukura, H. Yasuda, Y. Ohno and H. Ohno, Physica E **7**, 981 (2000).

[15] I.K. Kikoin, N.A. Babushkina, and T.N. Igosheva, Fizika Metallov i Metallovedenie [in Russian] **10**, 488 (1960).

[16] B.A. Aronzon, D.Yu. Kovalev, and A.N. Lagar'kov *et al.*, JETP Lett. **70**, 90 (1999).

[17] A. Gerber, A. Milner, M. Karpovsky *et al.*, J. Magn. Magn. Mater. **242-245**, 90 (2002).

[18] T. Wojtowicz, W.L. Lim, X. Liu, M. Dobrowolska, J.K. Furdyna, K.M. Yu, W. Walukiewicz, I. Vurgaftman, and J.R. Meyer, Appl. Phys. Lett. **83**, 4220 (2003).

[19] H. Luo, G.B. Kim, M. Cheon, X. Chen, M. Na, S. Wang, B.D. McCombe, X. Liu, Y. Sasaki, T. Wojtowicz, J.K. Furdyna, G. Boishin, and L.J. Whitman, Physica E **20**, 338 (2004).

[20] H. Ohno, D. Chiba, F. Matsukura, T. Omiya, E. Abe, T. Dietl, Y. Ohno, and K. Ohtani, Nature **408**, 944 (2000); F. Matsukura, D. Chiba, T. Omiya, E. Abe, T. Dietl, Y. Ohno, K. Ohtani, and H. Ohno, Physica E **12**, 351 (2002).

[21] B.A. Aronzon, A.B. Granovsky, A.B. Davydov, Yu.A. Danilov, B.N. Zvonkov, V.V. Ryl'kov, and E.A. Uskova, Phys. Solid State **49**, 171 (2007).

[22] B.A. Aronzon, M.V. Kovalchuk, E.M. Pashaev *et al.*, arXiv condmat 07080056.

[23] V.A. Gergel' and R.A. Suris, JETP **75**, 191 (1978).

[24] S.Y. Liu and X.L. Lei, Phys. Rev. B **72**, 195329 (2005).

[25] V.K. Dugaev, P. Bruno, M. Taillefumier, B. Canals, and C. Lacroix, Phys. Rev. B **71**, 224423 (2005).

[26] T. Dietl, F. Matsukura, H. Ohno, J. Cibert, and D. Ferrand, In: *Recent Trends in Theory of Physical Phenomema in High Magnetic Fields*, Ed.: I.D. Vagner (Kluwer, Dordrecht, 2003), p. 197; preprint condmat/0306484.

[27] P. Fumagalli, G. Sommer, H. Lippitz, S. Haneda, and H. Munekata, JAP **89**, 7015 (2001).

[28] I.F. Voloshin, A.V. Kalinov, S.E. Savel'ev, L.M. Fisher, N.A. Babushkina, L.M. Belova, D.I. Khomskii, and K.I. Kugel, JETP Lett. **71**, 106 (2000).

[29] S.V. Vonsovskii, *Magnetism* (Wiley, New York, 1974).

[30] S.V. Gudenko, B.A. Aronzon, and V.A. Ivanov, JETP Lett. **82**, 532 (2005).